An Epoxy Based Lignosulphonate Doped Polyaniline-Poly(Acrylamide Co-Acrylic Acid) Coating for Corrosion Protection of Aluminium Alloy 2024-T3

Gunjan Gupta[1,2,3,], Nick Birbilis[2] and A.S. Khanna[3]*

[1] IITB-Monash Research Academy, IIT Bombay
[2] Department of Materials Engineering, Monash University, Australia
[3] Department of Metallurgical Engineering and Materials Science, IIT Bombay, Powai, Mumbai, Maharashtra, 400076, India,
[*]E-mail: ggup6@student.monash.edu, gunjan.iitb@iitb.ac.in

Corrosion protection arising from epoxy coatings incorporating lignosulfonate-doped polyaniline-poly(acrylamide co-acrylic acid) (Pani-PAmAc) upon AA2024-T3 was studied in 3.5% NaCl. Synthesised Pani-PAmAc particles were investigated using TEM, FTIR, TGA and conductivity, whilst coatings were also physically examined using SEM. The corrosion performance of coatings was studied using a combination of potentiodynamic polarisation, EIS, and salt spray test. Results reveal that the epoxy based Pani-PAmAc coating was smooth and continuous. Potentiodynamic polarisation, EIS and salt spray testing revealed significant corrosion protection even after 50 days exposure to a 3.5% NaCl environment. This was attributed to the synergistic effect of polyaniline with poly(acrylamide co-acrylic acid) which prevented dopant loss and maintained electronic conduction even after long term exposure to a corrosive environment.

1. INTRODUCTION

The corrosion protection of aluminium alloy AA2024-T3, which is commonly used in aerospace applications, is typically achieved by the use of chromate coatings [1]. The aerospace industry places a high demand on coatings used to paint or repaint existing components. Several coating layers are used to provide improved adhesion, environmental and corrosion protection, visual aesthetics and low observability [2]. Although the performance of chromate based systems for corrosion protection is exceptionally good, there is increasing pressure to find replacements due to

environmental and health concerns [3]. Of the various alternatives, the use of conducting polymers (CPs) such as polyaniline, polypyrrole and polythiophene, as part of a corrosion resistant coating have been deemed potentially viable solutions [4-6]. Such coatings have also been purported to contribute to protecting internal components of the aircraft by minimising the electrical thundering effect [7]. Several methodologies have been proposed for the application of conducting polymer coatings, such as a primer alone, as a primer with conventional top coat, as an additive to paint formulations, or blending with conventional polymer coatings. Polyaniline has played a significant role in corrosion protection because of its high environmental stability, low cost and simple polymerisation process. One drawback with these materials is their low solubility, caused by π stacking of conjugation, resulting in poor processability in the finished polymers [8-10].

In the case of polyaniline, the use of dopants such as HCl and H_2SO_4 produces materials with high conductivity but with limited solubility. Replacing these dopants with larger functionalised organic dopants such as 10-camphorsulfonic acid (CSA), dodecylbenzenesulfonic acid (DBSA) and lignosulfonic acid (LGS) increases the solubility of conventional conducting polymer. Lignosulfonate (LGS) is a byproduct from pulp processing industries [11]. It has an aromatic network polymer which exhibits versatility in performance as a scale inhibitor, water reducer, dispersant and corrosion inhibitor [12-13]. An inherent lack of material stability comes from the fact that these dopants are easily lost due to heat, moisture, and rain water, from the conjugated polymers. Once the dopant is lost, the polymer loses its electrical conductivity and redox activity. The use of a copolymer along with conducting polymers addresses the problem of dopant loss whilst maintaining redox activity, electrical conductivity and the ability to impart corrosion resistance. Another aspect of conducting polymers is that they are typically hard, brittle solids, with very poor substrate adhesion. As such, this aspect is best addressed by blending the conducting polymer with a resin (epoxy, polyurethane, polyacrylate binder) to form a coating that can easily adhere to the surface of a substrate [14-15]. Racicot *et al*. used double-strand polyaniline for corrosion protection of aluminium. The double-strand Pani is a molecular complex of two polymers; (1) Pani and (2) a polyanion. These two linear polymers are bonded noncovalently in a side-by-side fashion to form a stable molecular complex. They reported that the rate of interfacial redox or charge transfer reaction could be relatively high compared to other solid coating because the material is electrically conductive [16-17].

The present work investigates the synthesis and the subsequent corrosion protection ability of epoxy based lignosulfonate doped polyaniline-poly (acrylamide co acrylic acid) (Pani-PAmAc) coatings applied to AA2024-T3. Synthesis of Pani-PAmAc particles was carried out by template guided chemical oxidative polymerisation method using LGS as dopant. Synthesised Pani-PAmAc particles were investigated using TEM, FTIR, TGA and conductivity. Pani and Pani-PAmAc was blended in epoxy resin and applied over AA2024-T3 aluminium. Surface morphology of the coatings was examined using SEM. The corrosion performance of coating was studied using a combination of potentiodynamic polarisation, EIS, and salt spray test.

2. EXPERIMENTAL

2.1 Materials

Aniline, acrylic acid, acryl amide, N,N'methylbisacrylamide, ammonium persulphate (APS) and lignosulfonic acid (LGS) were procured from Sigma Aldrich (India). Epoxy resin-bisphenol A (EEW 600) and polyamide hardener were obtained from Huntsman Chemicals (India). De-foamer (BYK A530), wetting agent (BYK 333) and dispersant (BYK 9076) were supplied by BYK chemicals (India). The AA2024-T3 alloy was procured from Airport Metals (Australia), with the nominal chemical composition shown in Table 1.

Table 1. Chemical composition (wt%) of AA2024-T3 aluminium alloy

Si	Fe	Cu	Mn	Mg	Cr	Zn	Ti	Al
0.07	0.16	4.19	0.62	1.40	0.01	0.07	0.03	Bal

2.2 Synthesis of Polyaniline-Lignosulfonate Particles (Pani-LGS)

It was found that the successful production of Pani-LGS was sensitive to synthesis variables such as concentrations, time and temperature. Significant effort was given to develop an optimised production, which is reported herein and a major outcome of the work. Pani-LGS was synthesised by the chemical oxidative polymerisation of aniline with ammonium persulfate (APS). 0.08 mole of aniline and 0.02 moles of LGS were dissolved in 200 ml of distilled water under stirring at room temperature for 6 hours. 98% sulphuric acid was added to attain a solution of pH=1. In the solution, 0.04 mole of APS in 100 ml distilled water was added drop wise under stirring at 0- 5°C for 5 hours and the mixed solution was stirred for 24 hrs at room temperature. The molar ratio of APS to aniline was maintained as 1:2. The colour of liquid changed to orange then to green after 5 hrs and finally to dark green colour at 24 hrs. Dark green colour ensures the complete polymerisation of aniline. The dark green solution was then filtered and washed with distilled water and methanol several times until the filtrate become colourless. The washed filtrate was then dried at 60^0C for 24 hrs [18].

2.3 Synthesis of Poly (acryl amide co-acrylic acid) microgel

PAmAc microgel was synthesized by using 0.05 mole acrylamide (Am), 0.003 mole acrylic acid (Ac), 0.002 mole N,N'methylbisacrylamide (MBA) (crosslinking agent) and 0.001 mole ammonium persulphate (APS) (oxidant) in 300 ml distilled water in a necked round bottom flask at $70^°$C under nitrogen atmosphere stirring at 300 rpm for 2 hrs. The transparent liquid converts to milky white microgel and this conversion indicates the completion of the reaction.

2.4 Synthesis of Polyaniline-Poly (acryl amide co-acrylic acid) [Pani-PAmAc] particles

Pani-PAmAc were synthesised via template guided chemical oxidative polymerisation of aniline in presence of LGS with poly (acryl amide co-acrylic acid) microgel using ammonium persulfate as an oxidant. PAmAc microgel was diluted with appropriate amount of water and stirred to form homogeneous solution. Then, 0.08 mole of aniline and 0.02 moles of LGS were added into the microgel solution under stirring at room temperature. 98% sulphuric acid was added to attain a solution of pH=1. To the solution, 0.04 mole of APS in 100 ml distilled water was added drop wise under stirring at 0- 5°C for 5 hours and the mixed solution was stirred for 24 hrs at room temperature. The molar ratio of APS to aniline was maintained as 1:2. The colour of liquid changed to orange then to green after 5 hrs and finally to dark green colour at 24 hrs. Dark green colour ensures the complete polymerisation of aniline. The dark green solution was then filtered and washed with distilled water and methanol several times until the filtrate become colourless. The washed filtrate was then dried at 60°C for 24 hrs [16, 19, 20].

2.5 Formulation of Coatings

An initial surface profile was achieved on the AA2024-T3 by abrading with 600 grit emery paper followed by 1200 grit. The samples were then conditioned by immersion in 5% NaOH of pH ~10 for 2 min to activate –OH group for adhesion, followed by distilled water rinsing and finally an acetone rinse to dry the surface The coatings were prepared by ultrasonic mixing of particles into epoxy matrix and xylene. This was further mixed with polyamide as curing agent and add 0.2 ml of de-foamer, wetting agent and dispersant as shown in Table 2.

Table2. Composition and Designation of Epoxy, Pani/Epoxy & Pani-PAmAc/Epoxy Coatings

Epoxy (gm)	Pani (gm)	Pani-PAmAc (gm)	Hardner (gm)	Additives (gm)	Xylene (ml)	Coating Designation
100	0	0	33.3	0.2-0.5	20	Epoxy
100	0.5	0	33.3	0.2-0.5	20	Pani
100	0	0.5	33.3	0.2-0.5	20	Pani-PAmAc

AA2024-T3 panels were coated with the formulated system and cured at room temperature for 12 hrs, followed by curing at 60^{0}C for 12 hrs. Epoxy and Pani-LGS coated samples were also prepared for comparing the results with Pani-PAmAc coated samples. The average dry coating thickness was

found to be 20±5 μm using an Elektrophysik coating thickness gauge (Model Exacto FN, Type 1800202).

2.6 Characterisation

FTIR spectra were recorded in the 4000-650 cm^{-1} with a Magna-IR spectrometer (550 Spectrometer, Nicolet). Transmission electron microscopy (TEM) was performed with a Philips CM200. Thermal behaviour was recorded by SDT Q600 v8.3 DSC-TGA Standard Instrument to evaluate weight change with respect to temperature at a heating rate of 10°C /min in the nitrogen atmosphere. A pellet of Pani-LGS and Pani-PAmAc (diameter: 10mm, thickness: 3mm) were prepared by compression at a 0.3 GPa at room temperature for conductivity measurement using a four-point probe (VEECO FPP-5000) meter.

The surface morphology of coated substrates was analysed via scanning electron microscopy (SEM) (Hitachi S3400N). Electrical conductivity was measured by Broadband Dielectric Spectrometer (BDS) provided by Novocontrol GmbH, Germany at temperature -50°C to 150°C with a step of 20°C and room temperature electrical conductivity was analysed using a four-point probe (VEECO FPP-5000) meter. Electrochemical studies were carried out by potentiodynamic polarisation and electrochemical impedance spectroscopy (EIS), using a Biologic VMP3 Potentiostat/Galvanostat. For electrochemical testing a three-electrode cell incorporating a saturated calomel reference electrode (SCE) and a platinum mesh counter electrode. The test area of the working electrode was in all cases 1 cm^2. All polarisation and EIS measurements preceded by immersion for 1 day prior to the electrochemical test in order to achieve potential and environmental stabilisation. EIS spectra were acquired in the frequency range from 10^6 Hz to 10^{-2} Hz with AC amplitude of 10 mV. The data were fit by EC Lab software. Corrosion resistance of coated panels was also examined by using salt spray test as per ASTM B117 specifications with 5wt% aqueous NaCl solution at 35 ± 2°C. Adhesion strength of coatings was measured according to ASTM D 3359-02 by the cross-cut technique.

3. RESULTS

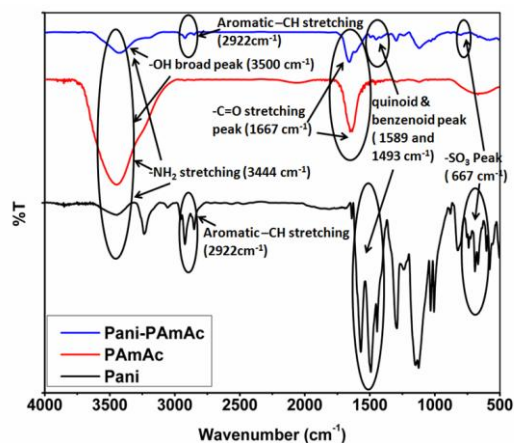### 3.1. Characterisation of Pani-LGS and Pani-PAmAc particles

Figure 1. FTIR Spectra of Pani, PAmAc and Pani-PAmAc particles

FTIR spectra of Pani, PAmAc and Pani-PAmAc are shown in Figure 1. The intense broad band near 3444 cm^{-1} and a medium intense band at 3236 cm^{-1} are attributed to the asymmetric and symmetric -NH$_2$ stretching modes, respectively. The peak observed at 2922 cm^{-1} was of an aromatic ---CH stretching. The bands at 1589 and 1493 cm^{-1} correspond to the quinoid and benzenoid ring stretching modes. The bands at 1291and 740 cm^{-1} are ascribed to in-plane and out-of-plane C---H bending modes, respectively. Peaks at 1291 and 1239 cm^{-1} correspond to ---NH bending and the symmetric component of the C---C (or C---N) stretching modes. The presence of the sulphate (SO$_3^-$) group was confirmed by the appearance of the band around 667 cm^{-1}. The FT-IR spectrum of PAmAc shows, broad peak in the region 3448 cm^{-1} was due to ---NH (amide) formed by partial hydrolysis of PAmAc. A strong sharp peak at 1652cm^{-1} was due to ---C=O group of acrylic acid. The peak observed at 1291 cm^{-1} was of aliphatic ---CH bending. The FT-IR spectrum of the Pani-PAmAc copolymer is somewhat similar to Pani, in which all the main vibration bands of PAmAc are overlapped with the bands of Pani, except for ---C=O group ($\approx$1667 cm^{-1}) and ---C-N group ($\approx$1031 cm^{-1}). Some vibrations in the range 1500–500 cm^{-1} are similar to those of Pani and few of them to those of PAmAc [11, 21].
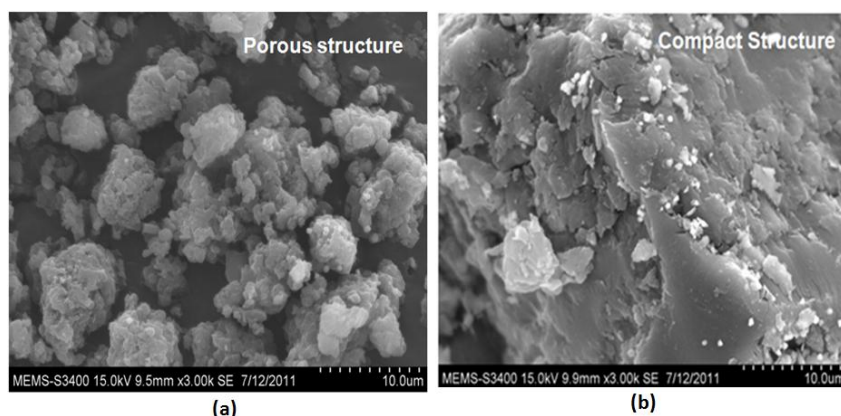

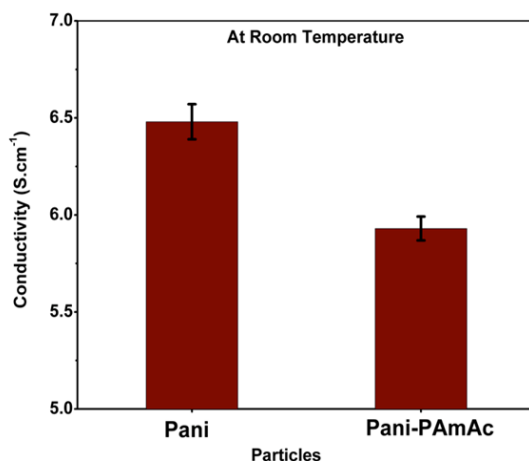**Figure 2.** SEM micrographs of (a) Pani-LGS (b) Pani-PAmAc particles

Figure 3. Electrical conductivity of Pani and Pani-PAmAc particles at room temperature

The SEM micrographs of Pani and Pani-PAmAc particles are shown in Figure 2 (a)-(b). Pani forms large aggregate consisting of many small particles whereas the surface of Pani-PAmAc was smooth and homogeneous. SEM micrograph shows that Pani was porous in nature that becomes compact when uniformly impregnated in the PAmAc microgel.

The room temperature conductivity of Pani and Pani-PAmAc particles were 6.48 S/cm and 5.94 S/cm, respectively as shown in Figure 3. It was found that the incorporation of copolymer (PAmAc) into Pani decreases the conductivity due to its insulating nature. Figure 4 shows the temperature dependence on electrical conductivity of Pani and Pani-PAmAc particles. The temperature dependent conductivity was measured from 223 K to 423K. The electrical conductivity of particles increases with increase in temperature due to thermal excitation of electrons.
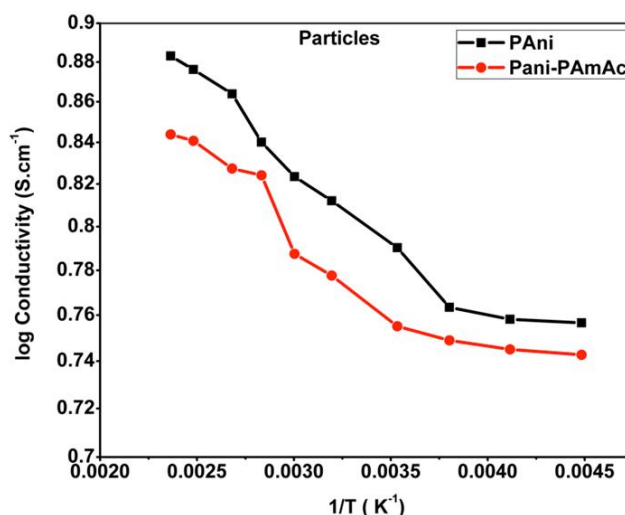

Figure 4. Logarithm of conductivity vs. inverse temperature for Pani and Pani-PAmAc particles

Three different steps of mass losses were observed from TGA analysis of Pani, PAmAc and Pani-PAmAc (Figure 5). For Pani, the initial loss, below170°C was assigned to loss of moisture. The second loss around 350°C was due to the thermo-chemical decomposition of the chemically active organic materials i.e. breaking of NH^+…..SO^{3-} interaction between Pani and LGS. Third stage was due to decomposition of chemical structure of polymeric polyaniline backbone at 600°C. For PAmAc, loss of moisture takes place at 40–200°C. The second loss was at 400°C, which corresponds to cyclisation of PAmAc chains and associated liberation of NH_3. The third loss was due to degradation at 400–500°C. For Pani-PAmAc, the initial mass loss was at 250°C, due to loss of moisture. The two major losses were observed 250–300°C and 300–400°C. The first decrease of mass was mainly due to the loss of lignosulfonate dopant whereas second loss was assigned to decomposition of PAmAc polymer. The final decomposition observed at 400–500°C was due to degradation of polymer. This overall confirms that the synthesised Pani-PAmAc has good thermal stability, better than that of Pani and PAmAc [12, 19].
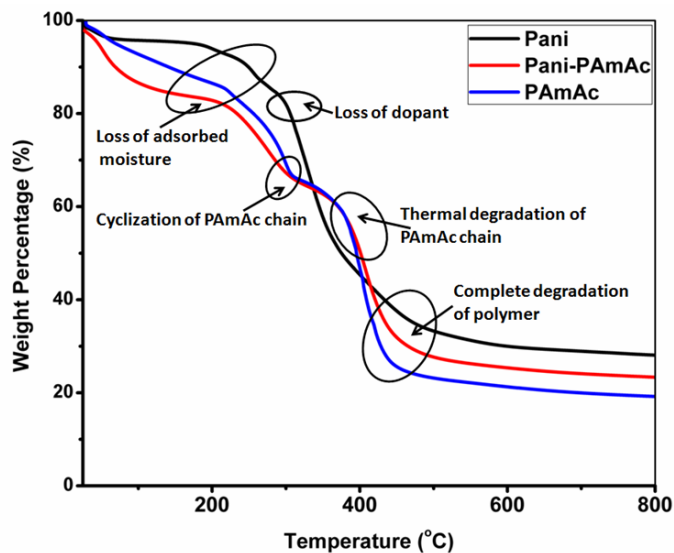
Figure 5. TGA curves of Pani, PAmAc and Pani-PAmAc particles
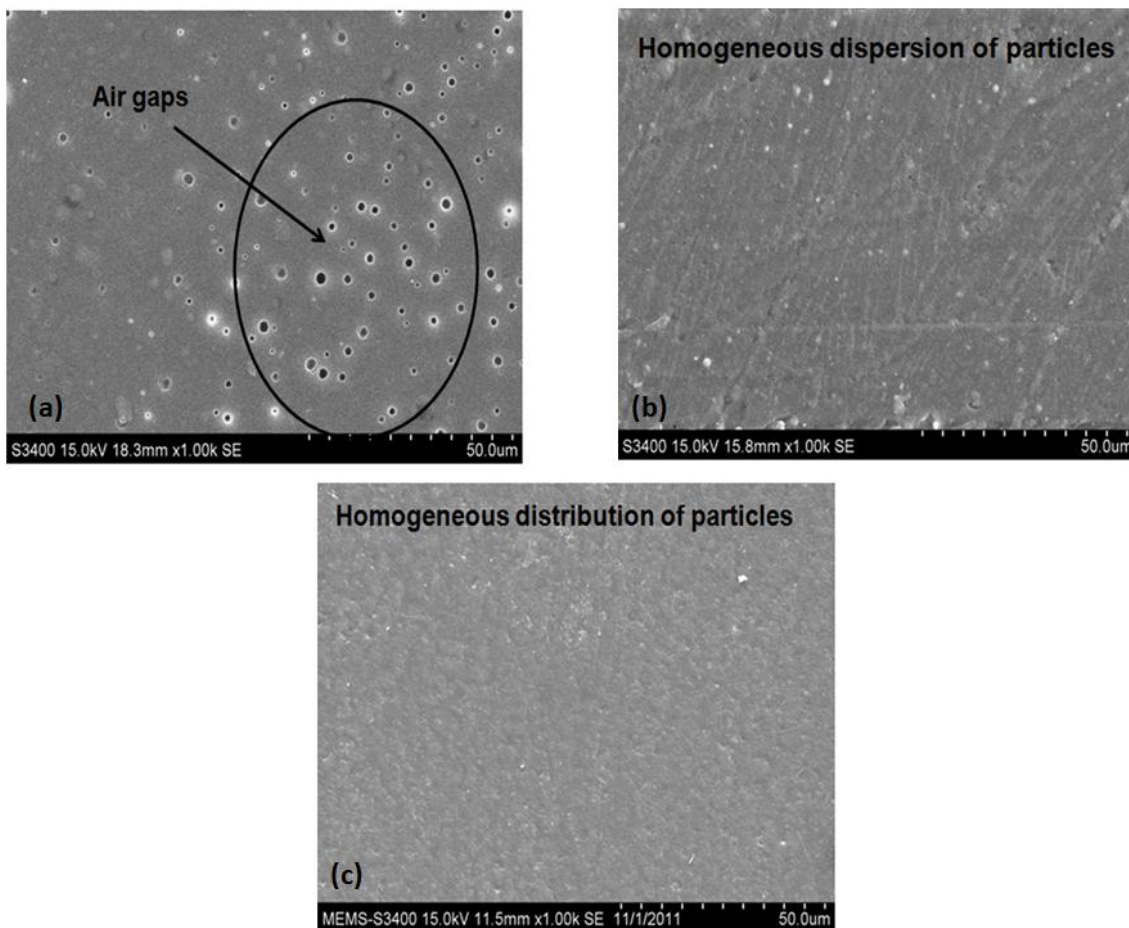
3.2 Surface Morphology of Coatings

Figure 6. SEM micrographs of (a) epoxy coating, (b) Pani-LGS coating, (c) Pani-PAmAc coatings
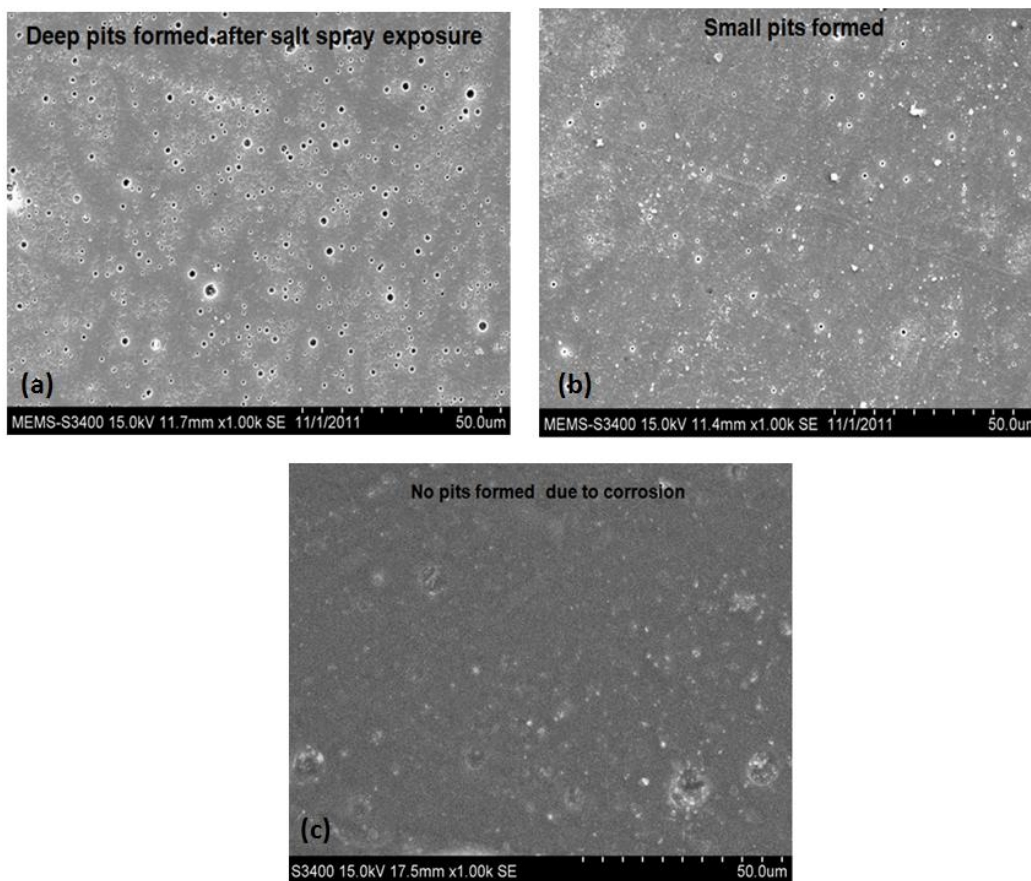
Figure 7. SEM micrographs of (a) epoxy, (b) Pani-LGS and (c) Pani-PAmAc coatings after 1200 hrs of salt spray exposure

The SEM micrographs of epoxy, Pani/Epoxy & Pani-PAmAc/Epoxy Coatings are seen in Figure 6(a)-6(c). Neat epoxy shows air gaps in the coating which continuously disappears on addition of Pani and Pani-PAmAc in epoxy matrix. Pani/Epoxy & Pani-PAmAc/Epoxy coatings exhibited smooth morphology and homogeneous dispersion of particles. Figure 7(a)-(c) shows SEM micrographs of epoxy, Pani/Epoxy & Pani-PAmAc/Epoxy Coatings coatings after 1200 hrs of salt spray exposure. Numerous large pits and surface damaged formed on the surface of epoxy, whereas very small pits formation on the Pani/Epoxy surface. However, Pani-PAmAc/Epoxy coating was compact and smooth in morphology – with no cracks and pits formed, even after 1200 hrs of salt spray exposure.

3.3 Electrical Conductivity of coatings

Table 3 shows the electrical conductivity of epoxy, Pani/Epoxy and Pani-PAmAc/Epoxy coatings. The electrical conductivity of epoxy coating was found in the range of 10^{-8} S/cm at room temperature. The conductivity of Pani/Epoxy was much higher as compared to epoxy due to conducting nature of polyaniline. A Pani-LGS particle forms the network of conducting particles in the

epoxy matrix. However, the conductivity of Pani-PAmAc/Epoxy coating slightly decreased due to insulating nature of PAmAc.

Table 3. Electrical conductivity of Epoxy, Pani/Epoxy and Pani-PAmAc/Epoxy coatings at room temperature

Coatings	Conductivity (S/cm)
Epoxy	10^{-8}
Pani/Epoxy	4.6
Pani-PAmAc/Epoxy	3.9

3.4 Corrosion performance of Coatings
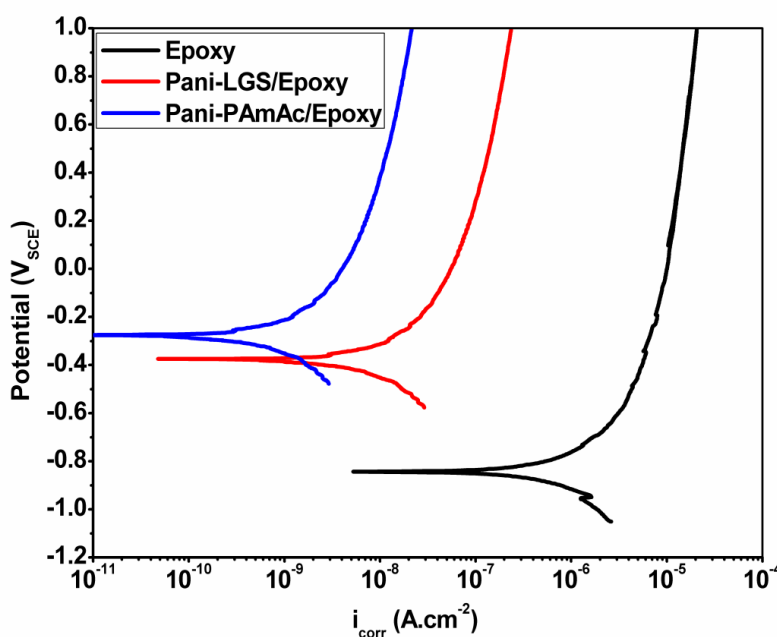
3.4.1 Potentiodynamic polarisation test

Figure 8. Potentiodynamic polarisation curves for epoxy, Pani-LGS and Pani-PAmAc coated A2024-T3 alloy in 3.5 % NaCl solution

The potentiodynamic polarisation curves for epoxy, Pani-LGS/Epoxy and Pani-PAmAc/Epoxy coated AA2024-T3 alloy were collected in 3.5% NaCl as shown in Figure 8. The corrosion protection of Pani-PAmAc coatings was attributed by shift in the potential to noble values in comparison to the epoxy and Pani-LGS coating in 3.5% NaCl. These noble potential shifts are regarded as the anodic protection potential. The results (Table 4) showed a decrease in corrosion current (i_{corr}) value for the Pani-PAmAc with respect to epoxy and Pani-LGS coated AA2024-T3. All polarisation curves show the insulating effect of epoxy, in that a distinct breakdown potential is not observed (unlike un-coated material), with current gently increasing with increasing anodic potentials [22]. The data reveal (from replicate testing) that the Pani-PAmAc/Epoxy resulted in consistently lower corrosion current being realised.

Table 4. Electrochemical Parameters of epoxy, Pani-LGS and Pani-PAmAc coated AA2024-T3 alloy in 3.5% NaCl solution

Compositions	OCP (mV_{SCE}) (Std. Dev.)	i_{corr} (A/cm^2) (Std. Dev.)	E_{corr} (mV_{SCE}) (Std. Dev.)
Epoxy	-813 (2.5)	2.61×10^{-6} (0.06)	-842 (1.3)
Pani-LGS/Epoxy	-354 (2.1)	5.13×10^{-8} (0.02)	-371 (1.2)
Pani-PAmAc/Epoxy	-274 (1.2)	3.31×10^{-9} (0.07)	-289 (0.6)

3.4.2 Electrochemical Impedance Spectroscopy (EIS)

To gain further insight into the corrosion protection afforded from the Pani-PAmAc coating, EIS was carried out, and the corresponding Bode plots shortly after immersion in 3.5% NaCl, after 30 days and after 50 days immersion in 3.5% NaCl are presented (Figures 9, Figure 10 and Figure 11). The low frequency value of $|Z|_{0.01}$ Hz for Pani-LGS coated AA2024-T3 alloy was found to be approximately four orders of magnitude higher than that of epoxy coated AA2024-T3 alloy. Interestingly however, for the Pani-PAmAc coating, the $|Z|_{0.01}$ Hz value was about five orders of magnitude higher than that of epoxy coated and about one order magnitude higher than that of Pani-LGS coating.
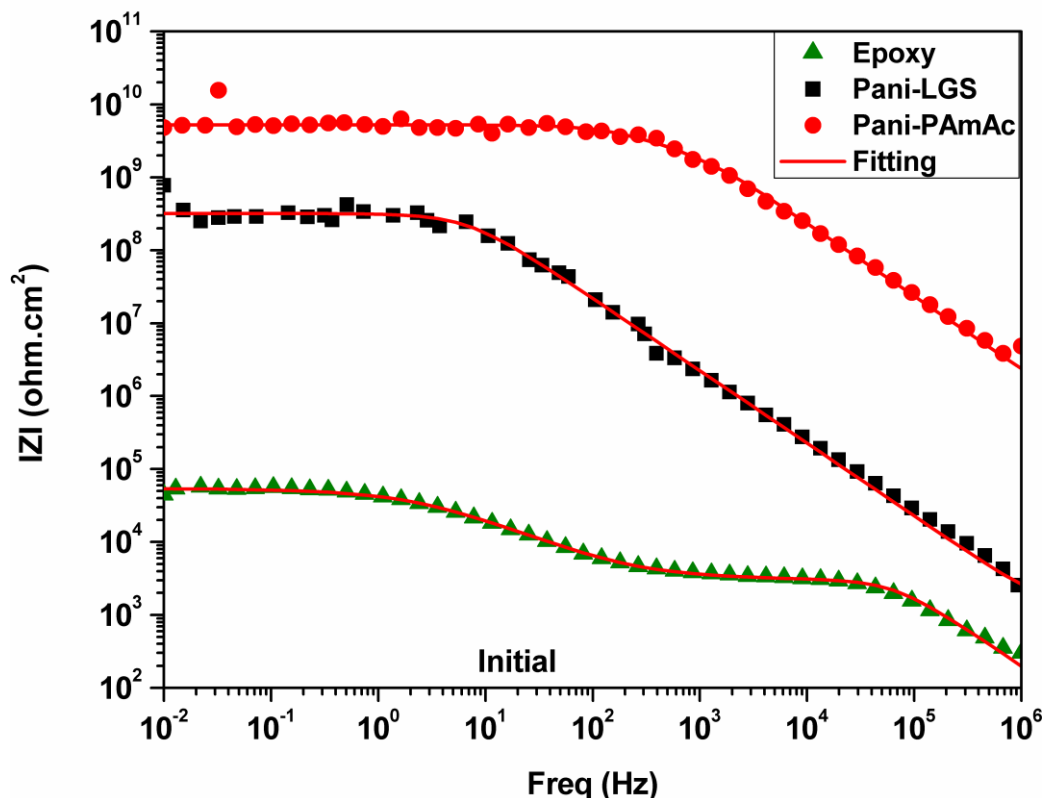

Figure 9. Impedance behaviour of epoxy, Pani-LGS and Pani-PAmAc coatings at initial period of immersion
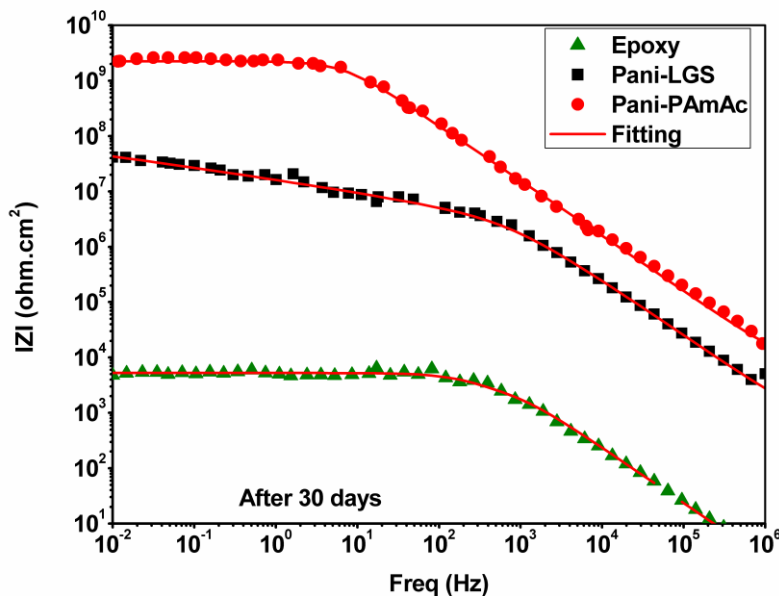
Figure 10. Impedance behaviour of epoxy, Pani-LGS and Pani-PAmAc coatings after 30 days of immersion
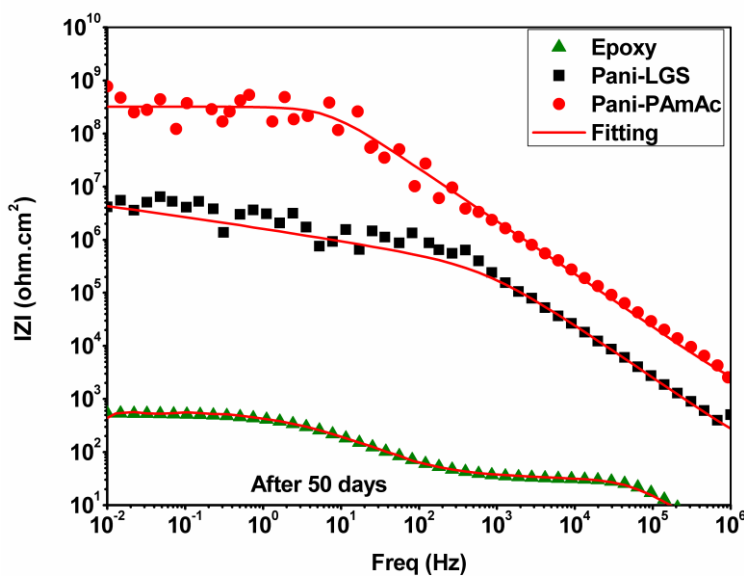

Figure 11. Impedance behaviour of epoxy, Pani-LGS and Pani-PAmAc coatings after 50 days of immersion

The increase in impedance value of Pani-PAmAc is ascribed to the PAmAc polymer which enhances the corrosion protection ability [23].

Following 30 days of immersion, the value of the low frequency impedance ($|Z|_{0.01\ Hz}$) for an epoxy and Pani-LGS coating decreased by an order of magnitude, whereas no significant change was observed for the Pani-PAmAc coating. After 30 days of constant immersion, an epoxy coating loses its potential to protect the substrate in 3.5% NaCl, with diffusion and water uptake through the coating has taken place. The bode plots exhibit systematic variations resulting from the changes in coating

resistance due to diffusion of chloride ions through the coating subsequently leading to corrosion of the AA2024-T3.

Following 50 days of immersion, the value of $Z|_{0.01\ Hz}$ for the Pani-LGS coating was decreased, indicating a diminished ability to protect the substrate. Following 50 days immersion, Pani-PAmAc coating revealed the highest impedance value of the coatings tested and showed protection ability in 3.5% NaCl.

By comparing the impedance values of the epoxy coating with those of the Pani-LGS and Pani-PAmAc coatings, the Pani-PAmAC coating provides about 3 orders magnitude greater impedance than epoxy and Pani-LGS coatings. This implies that the Pani-PAmAc coating is more protective as a corrosion barrier. The degradation of the coatings ability to impart corrosion resistance is often approximated by an acceptable corrosion protection performance being maintained when the coating resistance is greater than $\sim 10^7$ ohm.cm^2 [24-26]. The results herein indicate that the Pani-PAmAc coating provided the highest corrosion protection ability in saline water. It is also shown that the Pani-PAmAc coatings provide crack free and homogenous coatings upon the AA2024-T3, even after 1200 hours exposure (Figure 7). These images support electrochemical results, with the results also o validated by the salt spray test results, although both are completely different test.

3.5 Salt spray test

Pani-PAmAc/Epoxy coated AA2024-T3 shows, no sign of failure after 1200 hrs of exposure. However, Pani-LGS shows evidence of some small blisters and corrosion product formation beneath the coating surface. Epoxy coatings exhibited large blisters throughout the coating as shown in Figure 12. It was observed that Pani-PAmAc/Epoxy coating performs much better than Pani-LGS and Epoxy coatings. The high corrosion protection performance was due to PAmAc polymer which binds with polyaniline and maintains the electrical conductivity and corrosion protection efficiency even after long term exposure.
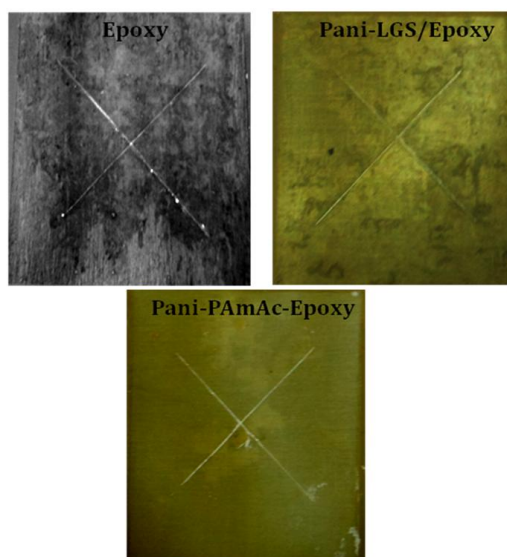

Figure 12. Salt spray photographs of Epoxt, Pani-LGS and Pani-PAmAc coating after 1200 hrs of exposure (6cm x 5cm)

3.6 Adhesion test

Table 5. Salt spray test and adhesion strength results of Epoxy, Pani/Epoxy and Pani-PAmAc/Epoxy Coatings

Compositions	Observations (After 1200 hrs exposure)	Adhesion Strength (ASTM D 3359) Before exposure	Adhesion Strength (ASTM D 3359) After 1200 hrs exposure
Epoxy	Large blisters throughout and few corrosion spots	5B	2B
Pani	Few small blisters (25% Area)	5B	3B
Pani-PAmAc	No signs of paint failure	5B	5B

High adhesion strength of the coatings is a basic requirement for good corrosion protection. The results of adhesion measurements by the crosshatch method are shown in Table 5. It is observed that the adhesion strength of Pani-PAmAc/Epoxy coatings were 5B, which is 'Excellent', prior to exposure to 3.5% NaCl. This was due to carboxylic acid present in PAmAc microgel which enhances the adhesion strength of the respective coatings with the substrate. The adhesion strength was also measured after 50 days exposure to 3.5% NaCl. It was observed that there was no effect on the adhesion strength of Pani-PAmAc/Epoxy coating. However, the adhesion strength of Pani-LGS/Epoxy coating decreased after 50 days immersion, which was due to generation of corrosion pits formed after long-term immersion. Epoxy and Pani-LGS/Epoxy coatings failed for long-term protection in aggressive environment.

4. DISCUSSION

The difficulties in using conventional conducting polymers for coatings are their lack of material stability, which comes from the dopants being easily lost due to heat, moisture and rain water. Once the dopant is lost, the polymer loses its electrical conductivity and its electroactivity. The synthesis of double stranded conducting polymer comprises a strand of conducting polymer complexed to a polyelectrolyte. Polyelectrolyte has two functional groups, carboxylic acid that balances the charge on the conducting polymer and provides adhesion with metal and another acrylamide group modify the physical and chemical properties of the polymer [16, 17]. The material stability is improved because the polymeric dopant is strongly coupled with the polyaniline chain, thus the dopants are not lost due to heat, moisture and rain water.
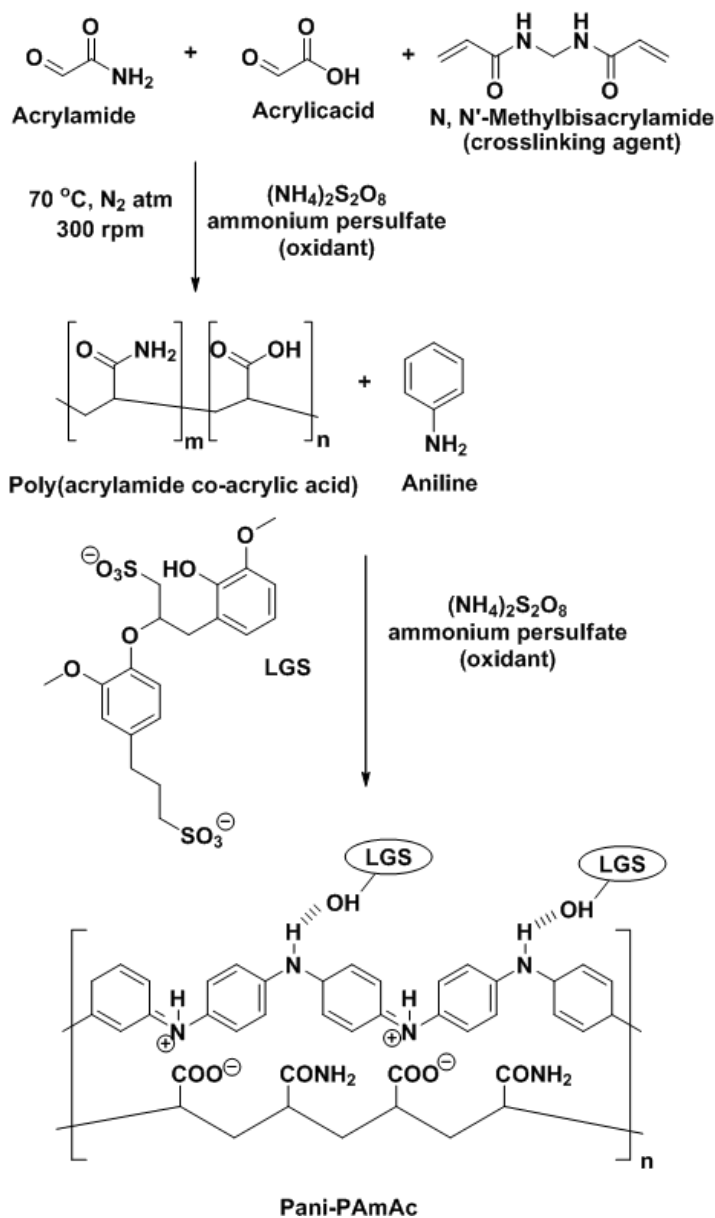
Figure 13. Schematic synthesis of lignosulphonate doped Polyaniline-Poly(acrylamide co-acrylic acid) [Pani-PAmAc]

Optimised concentration of chemicals, temperature and stirring speed (rpm) is necessary for the synthesis of poly (acrylamide co acrylic acid). On the excess addition of any chemical, the formation of the final microgel product is affected. On increasing the rpm to ~600 the chemical will convert to a white liquid, and no microgel (i.e. a sign of completion of reaction) was observed due to breaking of the polymer chain at higher rpm. Temperature also plays an important role in the formation of the polymer; at higher temperature polymer degradation takes place whereas at the lowest temperatures studied, the completion of the reaction is not possible. As such, an optimised temperature is required for satisfactory synthesis of the polymer.

The synthesised microgels (poly(acrylamide co acrylic acid)) were capable of forming a uniform dispersion in water media, and the active acidic groups present in the microgels adsorb the

monomer units of aniline and helped in the polymerization within the microgel environment itself and also promoted adhesion to metal substrates. In addition, the free polymerised particles present in the solvent were probably deposited over the micellar network, making the interaction more intimate [27]. This schematic diagram (Figure 13) shows how Pani-LGS is incorporating into a poly (acrylamide co acrylic acid) microgel structure and formed composites.

During polarisation of double stranded conducting polymer, deprotonation of the carboxylic group occurs resulting in a net negative charge in the conductive polymer. This was balanced to maintain electro neutrality [28]. One positive ion to balance the negative charge would be the Al^{+3} ions from dissolution of the substrate. The carboxylic ions in the conductive polymer would bind the aluminium ions in the passive layer in a fashion similar to the binding between multidentate polymer and a positively charged ion. An electrostatic attraction between the opposite polarity ions would stabilize the passive layer and essentially block the metal ions from penetrating through the conducting polymer [20]. The difficulty of the aluminium ions being dissolved in the solution is probably the reason for the formation of a tight and stable passive layer. A study by Sathiyanarayanan reported that the formation of the hydroxide layer provides protection to the metal and prevents it from continued corrosion [24, 29-32]. Whilst the polymer is in it its conducting (ES) form, it can provide protection to the metal and this can protection can persist whilst there are no defects in the coating [22]. The polarisation data indicate that the corrosion potential shifted to noble direction (anodic protection) which was due to a redox activity of Pani-PAmAc coating. Higher impedance of Pani-PAmAc coating was observed as compared to Pani-LGS. This could delay the diffusion of electrolyte through the coating. Even after 50 days immersion in 3.5% NaCl, Pani-PAmAc/Epoxy coating will able to provide corrosion protection to the metal - due to polyelectrolyte, which prevent from dopant loss and provide electrical conductivity to the polymer backbone. EIS results show that after 50 days immersion in 3.5% NaCl, impedance of epoxy and Pani-LGS coating reaches to very lower values, whereas Pani-PAmAc coating show still higher impedance values. Salt spray test and adhesion test results are also in support of this mechanism.

5. CONCLUSION

In the present work, the synthesis and subsequent corrosion resisting performance of epoxy based lignosulphonate doped Polyaniline-Poly(acrylamide co-acrylic acid) coating on aluminium alloy AA2024-T3 were studied. Successful synthesis was possible, and the complementary characterisation methods including SEM, potentiodynamic polarisation, adhesion and salt spray test revealed that epoxy based Pani-PAmAc coating was smooth and continuous, and capable of imparting significant corrosion protection. The important aspects of material synthesis were also given some specific attention. Potentiodynamic polarisation results indicated a high resistance to electrochemical reactions for Pani-PAmAc/epoxy coatings even after 50 days exposure to 3.5% NaCl; which was physically reconciled from salt spray test data. This was attributed to the synergistic effect of polyaniline with poly(acrylamide co-acrylic acid) which prevents dopant loss and maintains the electrical conductivity of the coating, even after long term exposure to a corrosive environment. The work also indicates

promise for optimisation of this class of coatings for enhanced corrosion protection and potential for further functionalisation to promote self healing aspects − which would be required in order to be a viable chromate replacement.

References

1. J. Zhao, G. Frankel and R. L. McCreery, *J. Electrochem. Soc.*, 145 (1998) 2258.
2. G. S. Frankel and R. L. McCreery, *Electrochem. Soc. Interface*, 10 (2001) 34.
3. R.L.Twite and G.P.Bierwagen, *Prog. Org. Coat.*, 33 (1998) 91.
4. D. E.Tallman, G. Spinks, A. Dominis and G. G.Wallace, *J. Solid State Electrochem.*, 6 (2002) 73.
5. M. Rohwerder and A. Michalik, *Electrochim. Acta*, 53 (2007) 1300.
6. P. Zarras and J. D. Stenger-Smith, An Introduction to Corrosion Protection using Electroactive polymer, *ACS Symposium Series*, Washington DC, 2003, Chapter 1, Vol.843, pp. 2–17
7. G.P. Bierwagen and D.E. Tallman, *Prog. Org. Coat.*, 41(2001) 201.
8. S. C. Yang and R. Brown, *Water borne polymeric complex and anti corrosive composition*, U.S. Patent No. US 6762238 B1 (2004).
9. A. Eftekhari, *Nanostructured Conductive Polymers*, Wiley, 2010, ISBN: 0470745851
10. D.E. Tallman, Y. Pae and G.P. Bierwagen, *Corrosion*, 56 (2000) 401.
11. L. Shao, J.H. Qiu, H.X. Feng, M.Z. Liu, G.H. Zhang, J.B. An, C. M. Gao and H. L. Lin, *Synth. Met.*, 159 (2009) 1761.
12. C. Yang and P. Liu, *Ind. Eng. Chem. Res.*, 48 (2009) 9498.
13. A. A. Chirkunov, Yu. J. Kuznetsov and M.A. Gusakova, *Prot. Met.*, 43 (2007) 367.
14. J. H. Huh, E.J.Oh and J.H.Cho, *Synth. Met.*, 153 (2005) 13.
15. J. Yun Kwon, E. Y. Kim and H. D. Kim, *Macromol. Res.*, 12 (2004) 303.
16. J.C. Seegmiller, J.E.Pereira da Silva, D.A.Buttry, S.I. Cordoba de Torresi and R.M. Torresi, *J. Electrochem. Soc.*, 152 (2005) B45.
17. R. Racicot, B. Richard and C. Y. Sze, *Synth. Met.*, 85 (1997) 1263.
18. M.R. Bagherzadeh, F. Mahdavi, M. Ghasemi, H. Shariatpanahi and H.R. Faridi, *Prog. Org. Coat.*, 68 (2010) 319.
19. C. Basavaraja, R. Pierson, T. K. Vishnuvardhan and D. S. Huh, *Eur. Polym. J.*, 44 (2008) 1556.
20. M. R. Mahmoudian, W. J. Basirun and Y. Alias, *Mater. Chem. Phys.,* 124 (2010) 1022.
21. F. Chen and P. Liu, *ACS Appl. Mater. Interfaces*, 3 (2011) 2694.
22. G.Gupta, N.Birbilis and A.S.Khanna, *Corros. Sci.*, 67(2013) 256.
23. M.G. Medrano-Vaca, J.G. Gonzalez-Rodriguez, M.E. Nicho, M. Casales and V.M. Salinas-Bravo, *Electrochim. Acta*, 53 (2008) 3500.
24. S. Sathiyanarayanan, S.S. Azim and G. Venkatachari, *Electrochim. Acta*, 52 (2007) 2068.
25. S. Chaudhari and P.P. Patil, *J. Appl. Polym. Sci.*, 106 (2007) 400.
26. M. Shabani Nooshabadi, S.M. Ghoreishi and M. Behpour, *Electrochim. Acta*, 54 (2009) 6989.
27. R. Racicot, M.N. Alias, R. Brown, R. L. Clark, H.B. Liu and S.C. Yang, *Mat. Res. Soc. Symp. Proc.*, 413 (1996) 529.
28. R.J.Racicot, R.L.Clark, H.B.Liu, S.C. Yang, M.N.Alias and R.Brown, *Proc. SPIE-Int. Soc. Opt. Eng.* 2528 (1995) 251.
29. A. Cook, A. Gabriel and N. Laycock, *J. Electrochem. Soc.*, 151 (2004) B529.
30. R.J. Holness, G. Williams, D.A. Worsley and H.N. McMurray, *J. Electrochem. Soc.*, 152 (2005) B73.

31. G.M. Spinks, A.J. Dominis, G.G. Wallace and D.E. Tallman, *J. Solid State Electrochem.*, 6 (2002) 85.
32. C.J. Weng, J.Y.Huang, K.Y.Huang, Y.S. Jhuo, M.H.Tsai and J.M.Yeh, *Electrochim. Acta*, 55 (2010) 8430.